

## Piezo- and photomodulated reflectivity spectra of ZnSe/GaAs and CdTe/InSb epilayers

Y. R. Lee and A. K. Ramdas

*Department of Physics, Purdue University, West Lafayette, Indiana 47907*

L. A. Kolodziejski and R. L. Gunshor

*School of Electrical Engineering, Purdue University, West Lafayette, Indiana 47907*

(Received 10 August 1988)

A lattice-mismatched ZnSe epilayer on a GaAs substrate and a near-lattice-matched CdTe epilayer on an InSb substrate grown by molecular-beam epitaxy (MBE) reveal sharp excitonic signatures in their piezo- and photomodulated reflectivity spectra. In the ZnSe/GaAs coherently grown thin epilayer (pseudomorphic film), the contraction parallel to the substrate surface is clearly revealed by the splitting of the valence-band maximum, as seen in the excitonic signatures. The deformation potential constants determined from the splittings and the shifts with respect to the stress-free bulk crystal are in excellent agreement with the bulk values. The MBE-grown CdTe epilayer in the CdTe/InSb heterostructure shows an exceptionally sharp excitonic signature close to that of the bulk.

### I. INTRODUCTION

In recent years, the growth of the group II-VI semiconductor heterostructures has attracted considerable attention thanks to their novel physical properties and a wide range of applications in optoelectronic devices. Among these, ZnSe and CdTe thin films on group III-V compound substrates are of particular interest because of their potential device application in the visible and near-infrared spectral region. Most of the studies deal with ZnSe epilayers grown on a GaAs substrate<sup>1</sup> and hence with a lattice mismatch between them. Thus both the epilayer and the substrate experience an interfacial strain. On the other hand, CdTe epilayers have been grown either on a lattice-mismatched GaAs (Ref. 2) or on a closely lattice-matched InSb (Ref. 3) substrate. The effect of the lattice mismatch on the optical properties of the ZnSe and CdTe thin films and the GaAs substrate have been previously investigated by reflectivity<sup>4</sup> and/or photoluminescence (PL).<sup>4,5</sup> It has been recently demonstrated that piezomodulated and photomodulated reflectivity spectra reveal the optical transitions associated with the electronic levels of semiconductor quantum-well heterostructures in an especially striking manner.<sup>6,7</sup> In this paper we report the study of the piezo- and the photomodulated reflectivity spectra of ZnSe/GaAs and CdTe/InSb epilayers and discuss them in the light of the physics of thin films and interfaces characteristics of semiconductor heterostructures.

### II. EXPERIMENT

The epilayers of cubic ZnSe studied in the present investigations were grown by molecular-beam epitaxy (MBE) either on a MBE-grown GaAs buffer layer, in turn grown on a (100) surface of a GaAs substrate, or on a GaAs substrate directly. In the CdTe/InSb heterostructure, a CdTe epilayer was produced on a MBE-grown

InSb buffer created on an InSb substrate.

The piezomodulation of the reflectivity spectrum of the crystals was accomplished by mounting the sample on a lead-zirconate-titanate transducer driven by a sinusoidal electric field with the field along its thickness. The alternating expansion and contraction of the transducer subjects the sample to an alternating strain with a typical rms value of  $\sim 10^{-5}$ . For comparison we have also recorded the photomodulated reflectivity spectrum of the samples. The photomodulation technique, described previously in the literature,<sup>8</sup> was accomplished by chopping the 6328-Å radiation from a 4.5-mW He-Ne laser incident on the specimen at 560 Hz. A glass optical cryostat was employed for low-temperature measurements. The sample-transducer combination was mounted on the cold finger of the optical cryostat, which provides thermal contact between the sample and the coolant. Such an arrangement yielded a sample temperature of above 20 K even when liquid helium was used as the coolant. For comparison, some of the photorefectivity spectra were recorded by replacing the transducer with a copper plate to improve thermal contact. The sample temperature then was close to 10 K with liquid helium as the coolant. A Perkin-Elmer (Model E-1) double-pass grating monochromator with a tungsten-halogen lamp as a source and a uv-enhanced Si photodiode constituted the spectrometer. The modulated part of the reflected radiation ( $\Delta R$ ) was detected and amplified by a phase sensitive lock-in amplifier. The signal, after digitizing, was processed with a microcomputer.

### III. EXPERIMENTAL RESULTS AND DISCUSSIONS

#### A. ZnSe epilayers

##### 1. Growth characteristics

The thicknesses of ZnSe films studied ranged from 0.1 to 2.3  $\mu\text{m}$ . It was found from both the evolution of

reflection high-energy electron diffraction (RHEED) patterns and RHEED intensity oscillations during the early stage of growth, that the films grown on GaAs epilayers exhibit two-dimensional nucleation characteristics, whereas three-dimensional nucleation is observed on the films grown on GaAs substrates.<sup>1</sup> In addition, cross-sectional transmission electron microscopy (TEM) measurements of the 0.1- $\mu\text{m}$  thick film show no dislocations or stacking faults in the film and its interface. We note that at room temperature lattice parameters of ZnSe and GaAs,  $a_{\text{ZnSe}} = 5.6684 \text{ \AA}$  (Ref. 9) and  $a_{\text{GaAs}} = 5.654 \text{ \AA}$  (Ref. 5), respectively, correspond to a 0.25% lattice mismatch. Coherent growth of ZnSe on the GaAs is accommodated by a two-dimensional contraction in the ZnSe epilayer parallel to the interface which allows the lattice spacing of ZnSe parallel to the interface to match that of GaAs; it was found that a ZnSe film with a thickness less than 0.15  $\mu\text{m}$  can be thus coherently grown on GaAs,<sup>1,10</sup> such films being referred to as "pseudomorphic." For thicker films a large density of dislocations is observed near the interface; the formation of the dislocations releases the strain due to the lattice mismatch and the film then has a lattice spacing approaching that of bulk ZnSe. It has been pointed out that the lattice spacing of ZnSe perpendicular to the interface becomes smaller than that of bulk for films thicker than 1  $\mu\text{m}$ .<sup>4</sup> This was attributed to the difference in the thermal contraction in the ZnSe epilayer and the GaAs substrate as the sample is cooled from the growth temperature to room temperature; the linear thermal expansion coefficient of ZnSe is larger than that of GaAs for  $T > 80 \text{ K}$  (Ref. 11). In the investigation reported in this paper we have studied excitonic signatures from both ZnSe and GaAs for a variety of ZnSe film thicknesses in order to discover and delineate the characteristics of the films described above.

## 2. The characterization of the strain and its effect on the electronic band structure

It is well known that the electronic band structure of semiconductors changes under an applied stress. In the absence of an external perturbation the electronic band structure of ZnSe and GaAs crystals has a twofold-degenerate  $\Gamma_6$  conduction-band minimum separated from a fourfold-degenerate  $\Gamma_8$  valence-band maximum by an energy gap  $E_g$  and a spin-orbit split twofold degenerate  $\Gamma_7$  state lying an energy  $\Delta_0$  below  $\Gamma_8$ ; all these band extrema occur at the center of the Brillouin zone. The effect of strain on the  $\Gamma_8$  band extremum can be expressed by the strain Hamiltonian<sup>12</sup>

$$H = -a \sum_{\alpha} \epsilon_{\alpha\alpha} - b \sum_{\alpha} \epsilon_{\alpha\alpha} (J_{\alpha}^2 - \frac{1}{3} J^2) - \frac{2}{\sqrt{3}} d \sum_{\substack{\alpha, \beta \\ \alpha < \beta}} \epsilon_{\alpha\beta} \{ J_{\alpha} J_{\beta} \}, \quad (1)$$

where  $\epsilon_{\alpha\beta}$  is a component of the strain tensor,  $\alpha, \beta = x, y$ , and  $z$  corresponding to the cubic axes,  $J$  is the angular momentum operator for  $J = \frac{3}{2}$ ,  $a$  is the hydrostatic pressure deformation potential,  $b$  and  $d$  are the shear deformation potentials, and  $\{ J_{\alpha} J_{\beta} \} = \frac{1}{2} (J_{\alpha} J_{\beta} + J_{\beta} J_{\alpha})$ . The

first term shifts the center of gravity of the entire  $\Gamma_8$  state, whereas the second and the third terms will split the fourfold multiplet into a twofold-degenerate  $m_j = \pm \frac{3}{2}$  state and a twofold-degenerate  $m_j = \pm \frac{1}{2}$  state for uniaxial stress along the [001] and [111] directions, respectively. We note that the strain does not remove the Kramers degeneracy. The  $\Gamma_6$  conduction band and the spin-orbit split  $\Gamma_7$  valence band experience only shifts, each characterized by a corresponding single, hydrostatic deformation-potential constant. Experimentally, under uniaxial stress, one observes a splitting of  $\Gamma_8$  (due to the shear strain) and a relative shift between  $\Gamma_6$  and  $\Gamma_8$  (due to the hydrostatic strain).

For the strained layer of ZnSe grown on a (100) surface of GaAs, the epilayer experiences both contraction in the plane (referred to as the  $xy$  plane) and an extension normal to the plane due to the lattice mismatch. The strain in the plane is given by

$$\epsilon = (a_{\parallel} - a_0) / a_0, \quad (2)$$

where  $a_{\parallel}$  is the effective lattice constant of the epilayer along the layer surface, and  $a_0$  is the lattice constant of bulk. The strain components are then given by

$$\begin{aligned} \epsilon_{xx} = \epsilon_{yy} = \epsilon, \quad \epsilon_{zz} = \frac{2s_{12}}{s_{11} + s_{12}} \epsilon, \\ \epsilon_{xy} = \epsilon_{yz} = \epsilon_{zx} = 0, \end{aligned} \quad (3)$$

where  $s_{11}$  and  $s_{12}$  are the elastic compliance constants. The energy change of the  $J = \frac{3}{2}$  state relative to the conduction-band minimum induced by the strain can be found by calculating the strain Hamiltonian matrix using the unperturbed  $J = \frac{3}{2}$  state wave functions,  $|\frac{3}{2}, \pm \frac{3}{2}\rangle$  and  $|\frac{3}{2}, \pm \frac{1}{2}\rangle$ . The energy shift with respect to its zero stress value for the interband transition associated with the  $p_{3/2}$  states, or equivalently of the exciton associated with the  $\Gamma_6$  and  $\Gamma_8$  band extrema, is thus given by

$$\Delta E_1 = \left[ 2a' \left( \frac{s_{11} + 2s_{12}}{s_{11} + s_{12}} \right) - b \left( \frac{s_{11} - s_{12}}{s_{11} + s_{12}} \right) \right] \epsilon \quad (4)$$

for  $|\frac{3}{2}, \pm \frac{3}{2}\rangle$  and

$$\Delta E_2 = \left[ 2a' \left( \frac{s_{11} + 2s_{12}}{s_{11} + s_{12}} \right) + b \left( \frac{s_{11} - s_{12}}{s_{11} + s_{12}} \right) \right] \epsilon \quad (5)$$

for  $|\frac{3}{2}, \pm \frac{1}{2}\rangle$ , where  $a'$  is the net hydrostatic potential constant characterizing the relative energy shift of  $\Gamma_6$  from  $\Gamma_8$  under the hydrostatic component and  $b$  the shear deformation-potential constant of  $\Gamma_8$  characterizing its splitting under the shear component, these being produced by the extension along [001].

## 3. Excitonic signatures

Figure 1 shows the piezomodulated reflectivity spectrum of a 0.1- $\mu\text{m}$  thick ZnSe pseudomorphic layer<sup>1</sup> in the spectral region of the ZnSe band edge. The spectrum is characterized by two distinct signatures at 2.8055 and 2.8195 eV. In order to determine the transition energy

accurately, we have performed a theoretical line-shape fitting, as shown in the inset; the description of the line-shape fitting is given in the Appendix. As can be seen, the fit is generally very good except for the relative intensities of the shoulders to the low-energy side of the prominent features. It appears that further refinement of the line shape may be necessary. (For the thicker epilayers the fits turned out to be superior.) It is known that the free exciton of bulk ZnSe has an energy of 2.802 eV at 4.2 K. The energy gap of semiconductors, as discussed, changes under stress. The feature at 2.8055 eV observed from the strained layer of ZnSe can be associated with the excitonic transition from the top of the valence band to the bottom of the conduction band if the energy shift induced by the strain is included. Two interpretations are possible for the feature at 2.8195 eV. (1) Photoluminescence excitation spectra of the ZnSe single crystal have revealed a signature at 2.817 eV at  $T \approx 4.2$  K (Ref. 13). The feature having an energy about 15 meV higher than that of the  $n=1$  free exciton of bulk ZnSe has been attributed to the  $n=2$  (excited state) free exciton. Based on this observation the feature at 2.8195 eV in Fig. 1 could then be attributed to the  $n=2$  free exciton, the one at 2.8055 eV then being the  $n=1$  free exciton. (2) As we have already discussed, the strain on the epilayer not only shifts the entire energy state, but also results in a splitting of the  $p_{3/2}$  valence band. The feature at 2.8195 eV, there-

fore, could then be alternately attributed to the excitonic transition associated with the  $|\frac{3}{2}, \pm\frac{1}{2}\rangle$  valence band whereas that at 2.8055 eV may be attributed to  $|\frac{3}{2}, \pm\frac{3}{2}\rangle$ .

The two alternate interpretations can be tested on the basis of the following observations. If both features observed in Fig. 1 were to be associated with the transitions originating from the top of the valence band, one would expect the 2.8055-eV feature to be significantly more pronounced than that at 2.8195 eV, since the oscillator strength of the excitonic transitions has  $n^{-3}$  dependence.<sup>14</sup> The relative intensity of the two features observed in the figure, however, does *not* support this interpretation. On the other hand, the piezomodulated reflectivity measurements can uniquely discriminate the excitonic transitions associated with the  $|\frac{3}{2}, \pm\frac{3}{2}\rangle$  and the  $|\frac{3}{2}, \pm\frac{1}{2}\rangle$  valence bands, respectively. We note that the intensity of the signature observed in the piezoreflectivity spectrum is proportional to the interband transition probability  $M_0$  and to the strain dependence of the energy shift,  $\partial E/\partial\epsilon$ . It is known that the ratio of  $M_0(|\frac{3}{2}, \pm\frac{3}{2}\rangle)$  to  $M_0(|\frac{3}{2}, \pm\frac{1}{2}\rangle)$  is 3 for a coplanar stress in a (100) surface<sup>15</sup> whereas the ratio of  $\partial E/\partial\epsilon(|\frac{3}{2}, \pm\frac{3}{2}\rangle)$  to  $\partial E/\partial\epsilon(|\frac{3}{2}, \pm\frac{1}{2}\rangle)$  deduced from Fig. 1 is  $\sim 0.2$  if the strain-split valence-band model is the correct interpretation. The product of  $M_0$  and  $\partial E/\partial\epsilon$  gives the relative intensity of the  $|\frac{3}{2}, \pm\frac{1}{2}\rangle$  feature to that of  $|\frac{3}{2}, \pm\frac{3}{2}\rangle$  to be  $\sim 1.7$ , in qualitative agreement with the experimental observation. A similar behavior is also observed in our piezomodulated reflectivity spectra of GaAs/ $\text{Al}_x\text{Ga}_{1-x}\text{As}$  quantum-well structures, in which the results from a single quantum well showed comparable intensities for the transitions associated with the  $|\frac{3}{2}, \pm\frac{1}{2}\rangle$  and  $|\frac{3}{2}, \pm\frac{3}{2}\rangle$  states.<sup>6</sup> To further confirm this interpretation we have also studied the photomodulated reflectivity spectrum of the same sample, in which the relative intensity of the spectrum is not sensitive to strain. The spectrum, displayed in Fig. 2, clearly shows that the feature at the lower energy position, presumably associated with the  $|\frac{3}{2}, \pm\frac{3}{2}\rangle$  state, is about three times stronger than the one at the higher energy position. The combination of the piezo- and the photomodulation techniques, therefore, allows us to identify the features associated with the heavy- and light-hole valence bands unambiguously. It is worth noting that the photomodulated reflectivity spectrum was recorded using the 6328-Å radiation from a He-Ne laser rather than with a source of photon energies  $\hbar\omega_L > E_g(\text{ZnSe})$ . This observation shows that, provided the epilayer is thin enough, the photoreflectivity spectrum of a semiconductor can be obtained with a pump beam with the photon energy lower than the energy gap of the crystal investigated. The only requirement is that the energy gap of the substrate be smaller than the photon energy of the pump beam; the modulation occurs at the interface.

Also observed in Fig. 1 is a weak feature at 2.834 eV. The feature, having an energy 14.5 meV higher than the 2.8195-eV feature, is attributed to the  $n=2$  free exciton of  $|\frac{3}{2}, \pm\frac{1}{2}\rangle$ . It is to be noted that the energies of both 2.8055- and 2.8195-eV features in Fig. 1 are slightly

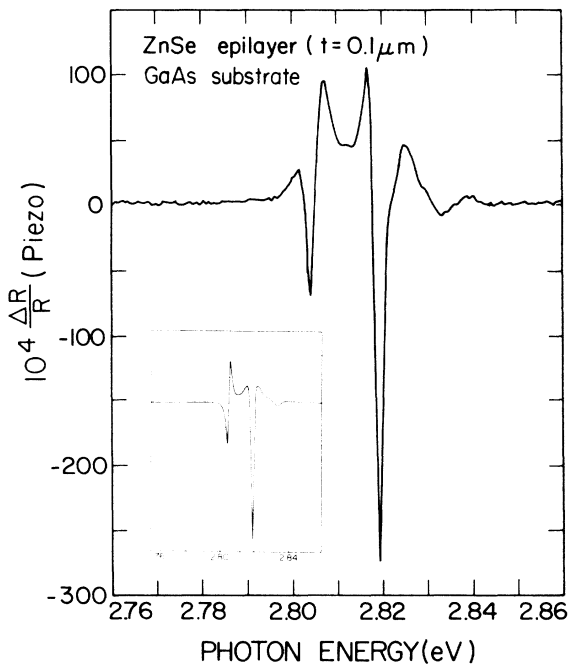


FIG. 1. Piezomodulated reflectivity spectrum of ZnSe/GaAs epilayer ( $t=0.1 \mu\text{m}$ ) for the spectral range in the vicinity of the free exciton of ZnSe. Liquid helium used as coolant. Sample was mounted on a transducer and the temperature was somewhat above 20 K. Also shown in the inset of the figure is a theoretical line-shape fitting using the first derivative of a Lorentzian function described in the Appendix.

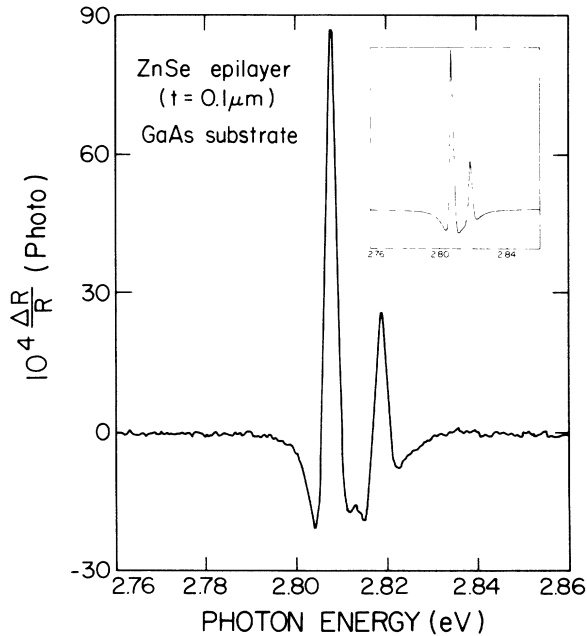


FIG. 2. Photomodulated reflectivity spectrum of the ZnSe/GaAs epilayer used to obtain the spectrum in Fig. 1. Liquid helium used as coolant. Sample was mounted on a copper plate and the temperature was about 10 K. The inset shows the theoretical line-shape fitting using the first derivative of a Lorentzian function. The chopped 6328-Å radiation from a He-Ne laser was used to produce the photomodulation.

different from those obtained from the photoreflectivity spectrum shown in Fig. 2 and those obtained from the PL measurements on a companion sample.<sup>1</sup> The lower energy ( $\sim 1$  meV) obtained for the feature associated with  $|\frac{3}{2}, \pm\frac{3}{2}\rangle$  in the piezoreflectivity spectrum, as compared with that of photoreflectivity and PL measurements, is due to the higher sample temperature in the piezoreflectivity measurements, whereas the larger splitting in the piezoreflectivity spectrum is attributed to the temperature dependence of the difference in the lattice constants; as a result the strain is temperature dependent.

Based on the model which invokes the valence-band splitting, we deduce<sup>16</sup> the values  $-5.26$  and  $-1.27$  eV for the deformation-potential constants  $a'$  and  $b$ , respectively, in good agreement with  $a' = -5.4$  and  $b = -1.2$  eV obtained for bulk ZnSe.<sup>17</sup> Also, these values are close to  $a' = -4.87$  eV and  $b = -1.05$  eV obtained from the PL data by Gunshor *et al.*<sup>1</sup>

The strain on the ZnSe layer is expected to decrease as the thickness of the films increases. Figure 3 shows the piezomodulated reflectivity spectrum of a 1.3- $\mu\text{m}$  thick ZnSe epilayer. The film has been grown on a GaAs substrate directly. The sharp feature at 2.8036 eV is associated with the excitonic transition from the  $\Gamma_8$  valence band to the  $\Gamma_6$  conduction band of ZnSe. The value is slightly higher than that obtained from the PL measurement<sup>1</sup> on a companion sample, which shows the  $n=1$  free-exciton signature at 2.802 eV. The origin of the small discrepancy between the result reported here and

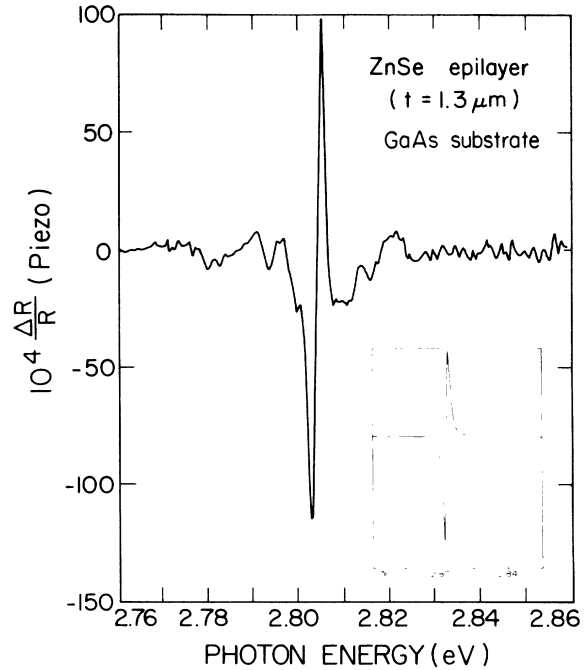


FIG. 3. Piezomodulated reflectivity spectrum of ZnSe/GaAs epilayer ( $t = 1.3 \mu\text{m}$ ) for the spectral range in the vicinity of the free exciton of ZnSe. Sample was cooled as in the measurement of Fig. 1. A theoretical line-shape fitting using the first derivative of a Lorentzian function is also in the inset.

the PL data is not clear. For films thicker than 2  $\mu\text{m}$  the piezomodulated reflectivity spectra reveal an additional signature at  $\sim 2.810$  eV. It has been pointed<sup>4</sup> out that the critical layer thickness for the formation of the dislocations is about 0.15  $\mu\text{m}$ . X-ray diffraction measurements<sup>4</sup> on films thicker than 0.15  $\mu\text{m}$  have revealed an additional diffraction peak at a lower diffraction angle than that of the main diffraction peak. The peak was attributed to the interface layer of ZnSe which has a lattice spacing almost the same as that of films thinner than 0.15  $\mu\text{m}$ . The layer thus suffers a two-dimensional contraction in the plane and an extension normal to the plane. The feature at 2.810 eV, therefore, could be attributed to the excitonic transition associated with the strained interface layer of ZnSe.

We have also investigated the electronic band structure of GaAs in this heterostructure with a lattice mismatch. Figure 4 shows the photomodulated reflectivity spectrum of the same sample used to obtain the result shown in Fig. 3. The spectrum, characterized by two signatures at 1.517 and 1.511 eV, was recorded for energies in the vicinity of the absorption edge of GaAs. Using the energy gap of 1.521 eV and the free-exciton binding energy of 4 meV for GaAs at 4.2 K, we identify the feature at 1.517 eV as the  $n=1$  free exciton of GaAs. The value, in excellent agreement with that of bulk GaAs, indicates that the GaAs layer is strain-free. The feature at 1.510 eV is attributed to a bound exciton; its energy is close to that of the feature associated with the exciton bound to a neutral Zn

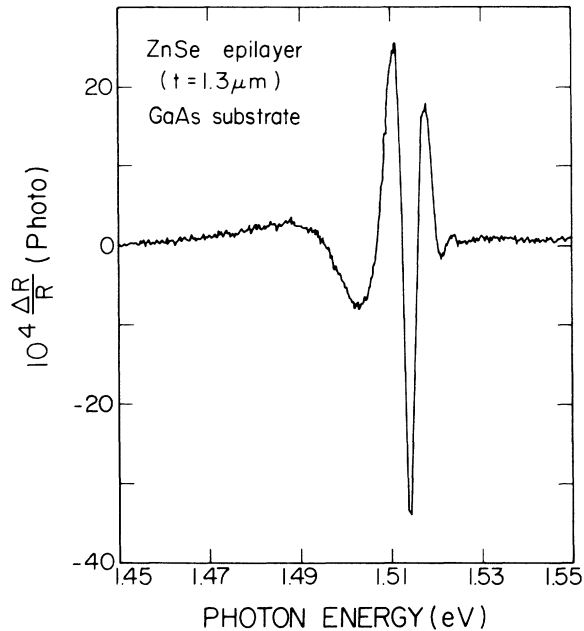


FIG. 4. Photomodulated reflectivity spectrum of the ZnSe/GaAs epilayer used to obtain the spectrum in Fig. 3. The spectrum recorded for the spectral range in the vicinity of the free exciton of GaAs. Sample was cooled as in the measurement of Fig. 2. The chopped 6328-Å radiation from a He-Ne laser was used to produce the photomodulation.

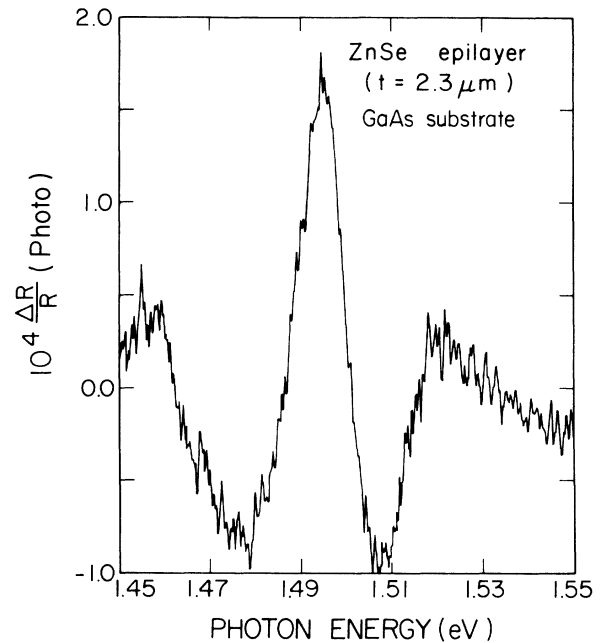


FIG. 5. Photomodulated reflectivity spectrum of ZnSe/GaAs epilayer ( $t = 2.3 \mu\text{m}$ ) for the spectral range in the vicinity of the free exciton of GaAs. Sample was mounted on a copper plate and liquid nitrogen was used as coolant. The chopped 6328-Å radiation from a He-Ne laser was used to produce the photomodulation.

acceptor observed in the PL spectrum of a Zn- and Se-doped *p*-type GaAs.<sup>18</sup> For thicker films the free-exciton energy of GaAs decreases. Figure 5 shows the photomodulated reflectivity spectrum in the spectral region of the GaAs absorption edge for a 2.3- $\mu\text{m}$  thick ZnSe film. Liquid nitrogen was used as a coolant. We attribute the feature at 1.494 eV to the free exciton of the GaAs substrate in the heterostructure. It is about 13 meV lower than that of bulk GaAs. In contrast to the relatively strain-free thick ZnSe epilayer in this heterostructure, the GaAs substrate appears to be under a two-dimensional extension in the plane and a uniaxial contraction normal to the plane. In the context of this two-dimensional stress, the feature at 1.494 eV can be interpreted as the excitonic transition associated with the  $|\frac{3}{2}, \pm\frac{3}{2}\rangle$  valence band. This shift corresponds to a planar tensile strain of 0.15%, based on the parameters in Ref. 5. The weaker  $|\frac{3}{2}, \pm\frac{1}{2}\rangle$  excitonic component is presumably not observed in view of the broad linewidths in these measurements.

### B. CdTe epilayers

The epilayer of CdTe studied has a thickness of 1.3  $\mu\text{m}$ . Figure 6 shows the piezomodulated reflectivity spectrum for the spectral range near the band edge of CdTe. The sharp feature at 1.5954 eV corresponds to the free exciton of CdTe. Two origins are possible for the feature at 1.5927 eV. (i) Barnes and Zanio<sup>19</sup> observed in the PL spectrum of In-doped CdTe a feature at 1.593 eV which they attributed to excitons bound to neutral donors. A

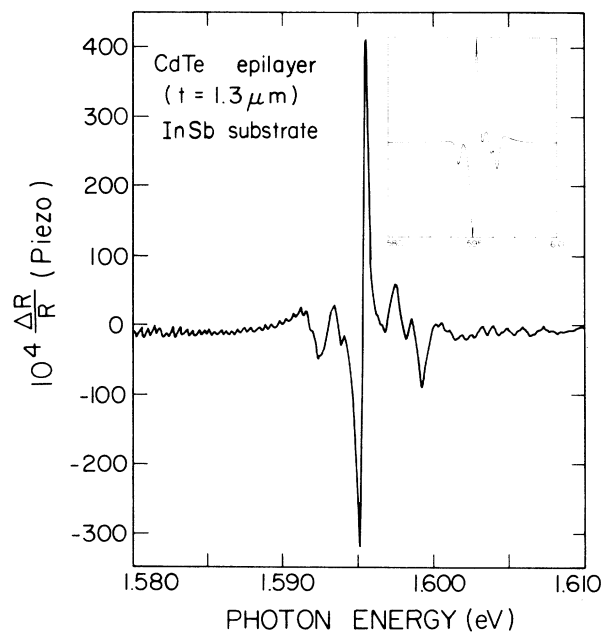


FIG. 6. Piezomodulated reflectivity spectrum of CdTe/InSb epilayer ( $t = 1.3 \mu\text{m}$ ) for the spectral range in the vicinity of the free exciton of CdTe. Sample was cooled as in the measurements of Figs. 1 and 3. A theoretical line-shape fitting using the first derivative of a Lorentzian function is also shown in the inset.

peak at the same position has also been observed by Leopold *et al.*<sup>20</sup> on MBE-grown CdTe/GaAs heterostructures; they also attributed that to a neutral donor-bound exciton. (ii) Recently, Feng *et al.*<sup>21</sup> have investigated the behavior of bound excitons of CdTe in MBE-grown CdTe/InSb heterostructures for different temperatures and sample preparation processes. On the basis of a lack of significant change in the intensity of the 1.593 eV feature in the PL spectra between 6.5 and 30 K, in contrast to that of excitons bound to chemical impurities (acceptors or donors), they concluded that it was not due to a donor-bound exciton. On the other hand, the feature becomes more intense after samples have undergone mechanical thinning, perhaps due to the introduction of mechanical damage. They, therefore, proposed that the feature at 1.593 eV is associated with an exciton bound to a mechanical-damage-induced defect, either a line defect such as a dislocation or a point-defect-impurity complex. The feature at 1.5983 eV, previously observed in very pure bulk CdTe (Ref. 22) and MBE-grown CdTe films,<sup>3,21</sup> has been attributed<sup>21</sup> to the upper branch of the polariton of the free exciton, a result of exciton-photon interaction. In the vicinity of the intersection of the photon and free-exciton dispersion curves, the exciton dispersion curve is altered and gives rise to three polariton branches for direct-gap zinc-blende semiconductors,<sup>23</sup> whose  $\Gamma_8$  valence band is fourfold degenerate. Such an exciton-photon interaction effect can only be observed in high quality samples. The feature at 1.5994 eV is presumably due to the excitonic transition associated with the  $|\frac{3}{2}, \pm\frac{1}{2}\rangle$  state arising from the interface layer, which is under a small two-dimensional contraction along the interface.

#### IV. CONCLUSIONS

We have demonstrated that the semiconductor heterostructures, in addition to their great potential for optoelectronic device applications, are systems of special interest in the context of basic physics. The lattice-mismatched heterostructures, for instance, provide a new approach in the study of deformation-potential constants of semiconductors. MBE-grown thin films can be structurally superior to the bulk, and hence many novel physical phenomena become accessible when studied with them, i.e., excitonic polaritons. Piezo- and photo-modulated reflectivity, as illustrated in this paper, are sensitive experimental techniques in the study of excitations associated with the epilayer, the interface, and the substrate. Several aspects of the present study need further investigation, e.g., the significant change in the strain present in the GaAs substrate for the ZnSe film with thickness in the range 1.3 and 2.3  $\mu\text{m}$  is not fully understood. Further work is in progress.

#### ACKNOWLEDGMENTS

The work reported in this investigation received support from the National Science Foundation–Materials Research Group No. DMR-85-20866 as well as the Defense Advanced Research, Projects Agency-University Research Initiative consortium on “Diluted Magnetic

Semiconductors and their Heterostructures,” administered by the office of Naval Research, Grant No. N00014-86-K-0760.

#### APPENDIX

In the piezomodulated reflectivity experiments, the normalized change in the reflectivity, without taking into account the multiple internal reflection, can be expressed by

$$\frac{\Delta R}{R} = A \frac{\partial \epsilon_1(\omega)}{\partial \omega_0} \Delta \omega_0 + B \frac{\partial \epsilon_2(\omega)}{\partial \omega_0} \Delta \omega_0, \quad (\text{A1})$$

where  $A$  and  $B$  are the so-called Seraphin coefficients,<sup>24</sup> and  $\epsilon_1(\omega)$  and  $\epsilon_2(\omega)$  are the real and imaginary parts of the dielectric constant, respectively, and  $\Delta \omega_0$  is either the change of the energy gap (band-to-band transition) or the change of the exciton energy (excitonic transition) due to the modulation. For semiconductors  $B$  is usually much smaller than  $A$  in the vicinity of the fundamental absorption edge.<sup>24</sup> The line shape of  $\Delta R/R$  obtained in the piezomodulated reflectivity measurements, therefore, is dominated by the first derivative of the real part of the dielectric function.

In the case of an epilayer on a substrate the reflectivity of the sample is given by

$$R_t = R_1 + \frac{R_2(1-R_1)^2 e^{-2\alpha t}}{1-R_1 R_2 e^{-2\alpha t}}, \quad (\text{A2})$$

where  $R_1$  and  $R_2$  are the reflectivities of the epilayer with respect to vacuum and the substrate, respectively, and  $t$  and  $\alpha$  are the thickness and the absorption coefficient of the epilayer, respectively. The normalized change in the reflectivity is then given by

$$\begin{aligned} \frac{\Delta R_t}{R_t} = & \left[ \frac{1-R_t}{1-R_1} \right]^2 \frac{\Delta R_1}{R_1} + \frac{R_t-R_1}{R_t} \left[ 1 + \frac{R_1(R_t-R_1)}{(1-R_1)^2} \right] \\ & \times \left[ \frac{\Delta R_2}{R_2} - 2(t\Delta\alpha + \alpha\Delta t) \right]. \end{aligned} \quad (\text{A3})$$

Near the absorption edge of the epilayer, the quantities  $\Delta R_2/R_2$  and  $\alpha\Delta t$  are insignificant compared with  $t\Delta\alpha$  and Eq. (A3) can be simplified as

$$\frac{\Delta R_t}{R_t} \approx \frac{\Delta R_1}{R_1} + \frac{R_t-R_1}{R_t} (-2t\Delta\alpha). \quad (\text{A4})$$

with

$$\Delta\alpha \sim (\omega/c)\epsilon_1^{-1/2} \frac{\partial \epsilon_2(\omega)}{\partial \omega_0} \Delta \omega_0. \quad (\text{A5})$$

$\epsilon_{e1}$  and  $\epsilon_{e2}$  are the real and imaginary parts of the dielectric function of the epilayer respectively. The line shape of  $\Delta R/R$  for an epilayer, therefore, is determined by the first derivative of the real and imaginary parts of the dielectric function.

For interband transitions, the first derivative of the dielectric functions near the  $M_0$  type of the three-dimensional critical point is given by<sup>25</sup>

$$\frac{d\epsilon_1(\omega)}{d\omega_g} \propto -\frac{1}{2}\Gamma^{-1/2} \frac{[(x^2+1)^{1/2}-x]^{1/2}}{(x^2+1)^{1/2}} \quad (\text{A6})$$

and

$$\frac{d\epsilon_2(\omega)}{d\omega_g} \propto -\frac{1}{2}\Gamma^{-1/2} \frac{[(x^2+1)^{1/2}+x]^{1/2}}{(x^2+1)^{1/2}} \quad (\text{A7})$$

with  $x = (\omega - \omega_g)/\Gamma$ .  $\Gamma$  is the broadening parameter. For excitonic transitions, they are given by<sup>25</sup>

$$\frac{d\epsilon_1(\omega)}{d\omega_0} \propto -\Gamma^{-2} \left[ \frac{x^2-1}{(x^2+1)^2} \right], \quad (\text{A8})$$

and

$$\frac{d\epsilon_2(\omega)}{d\omega_0} \propto -\Gamma^{-2} \left[ \frac{-2x}{(x^2+1)^2} \right], \quad (\text{A9})$$

where  $x = (\omega - \omega_0)/\Gamma$ .

- <sup>1</sup>R. L. Gunshor, L. A. Kolodziejski, M. R. Melloch, M. Vaziri, C. Choi, and N. Otsuka, *Appl. Phys. Lett.* **50**, 200 (1987).  
<sup>2</sup>L. A. Kolodziejski, R. L. Gunshor, N. Otsuka, X.-C. Zhang, S.-K. Chang, and A. V. Nurmikko, *Appl. Phys. Lett.* **47**, 882 (1985); see also L. A. Kolodziejski, R. L. Gunshor, N. Otsuka, S. Datta, W. M. Becker, and A. V. Nurmikko, *IEEE J. Quantum Electron.* **QE-22**, 1666 (1986).  
<sup>3</sup>R. F. C. Farrow, G. R. Jones, G. M. Williams, and I. M. Young, *Appl. Phys. Lett.* **39**, 954 (1981).  
<sup>4</sup>Takafumi Yao, Yasumasa Okada, Susumu Matsui, Kohtaro Ishida, and Isao Fujimoto, *J. Cryst. Growth* **81**, 518 (1987).  
<sup>5</sup>D. J. Olego, J. Petruzzello, S. K. Ghandhi, N. R. Taskar, and I. B. Bhat, *Appl. Phys. Lett.* **51**, 127 (1987).  
<sup>6</sup>Y. R. Lee, A. K. Ramdas, F. A. Chambers, J. M. Meese, and L. R. Ram Mohan, *Appl. Phys. Lett.* **50**, 600 (1987).  
<sup>7</sup>O. J. Glembocki, B. V. Shanabrook, N. Bottka, W. T. Beard, and J. Comas, *Appl. Phys. Lett.* **46**, 970 (1985); P. Paray-anthal, H. Shen, Fred H. Pollak, O. J. Glembocki, B. V. Shanabrook, and W. T. Beard, *Appl. Phys. Lett.* **48**, 1261 (1986).  
<sup>8</sup>R. E. Nahory and J. L. Shay, *Phys. Rev. Lett.* **21**, 1569 (1968).  
<sup>9</sup>S. Larach, R. E. Shrader, and C. F. Stocker, *Phys. Rev.* **108**, 587 (1957).  
<sup>10</sup>Hiroshi Mitsuhashi, Iwao Mitsuishi, Masashi Mizuta, and Hiroshi Kukimoto, *Jpn. J. Appl. Phys.* **24**, L578 (1985).  
<sup>11</sup>S. I. Novikova, *Semiconductors and Semimetals*, edited by R. K. Willardson and A. C. Beer (Academic, New York, 1966),

Vol. 2, p. 33.

- <sup>12</sup>See, for example, E. P. Kartheuser, S. Rodriguez, and P. Fisher, *Phys. Status Solidi B* **64**, 11 (1974).  
<sup>13</sup>P. J. Dean and D. C. Herbert, *Phys. Rev. B* **23**, 4888 (1981).  
<sup>14</sup>R. J. Elliott, *Phys. Rev.* **108**, 1384 (1957).  
<sup>15</sup>H. Mathieu, D. Auvergne, and J. Camassel, *Phys. Status Solidi B* **58**, 227 (1973).  
<sup>16</sup>We have used the elastic stiffness constants of ZnSe,  $c_{11}$ , and  $c_{12}$ , given by C. G. Hodgins and J. C. Irwin, *Phys. Status Solidi A* **28**, 647 (1975).  
<sup>17</sup>A. Blacha, H. Presting, and M. Cardona, *Phys. Status Solidi B* **126**, 11 (1984).  
<sup>18</sup>M. A. Gilleo, P. T. Bailey, and D. E. Hill, *Phys. Rev.* **174**, 898 (1968).  
<sup>19</sup>C. E. Barnes and K. Zanio, *J. Appl. Phys.* **46**, 3959 (1975).  
<sup>20</sup>D. J. Leopold, J. M. Ballingall, and M. L. Wroge, *Appl. Phys. Lett.* **49**, 1473 (1986).  
<sup>21</sup>Z. C. Feng, M. G. Burke, and W. J. Choyke, *Appl. Phys. Lett.* **53**, 128 (1988).  
<sup>22</sup>P. Hiesinger, S. Suga, F. Willmann, and W. Dreybrodt, *Phys. Status Solidi B* **67**, 641 (1975).  
<sup>23</sup>G. Fishman, *Solid State Commun.* **27**, 1097 (1978).  
<sup>24</sup>B. O. Seraphin and N. Bottka, *Phys. Rev.* **145**, 628 (1966).  
<sup>25</sup>Bruno Batz, *Semiconductors and Semimetals*, edited by R. K. Willardson and A. C. Beer (Academic, New York, 1972), Vol. 9, p. 315.